Comparison of hydrogel- and xerogel-based sorbent from Empty Fruit Bunch (EFB)

A.B. Alias [a,*], D. Qarizada [a,b], N.S.A. Malik [a], N.M.R. Noraini [a,c], Z.A. Rashid [a]

[a] Industrial Process Reliability & Sustainability (INPRES) Research Group, School of Chemical Engineering, College of Engineering, Universiti Teknologi MARA, Shah Alam, 40450 Selangor, Malaysia

[b] Faculty of Chemical Engineering, Jawzjan University, Jawzjan, Afghanistan

[c] National Institute of Occupational Safety & Health (NIOSH), Bandar Baru Bangi, 43650 Selangor, Malaysia

* Corresponding e-mail address: azilbahari@uitm.edu.my

ORCID identifier: https://orcid.org/0000-0002-6217-7392 (A.B.A.)

ABSTRACT

Purpose: This paper focuses on the synthesis and comparison of hydrogel- and xerogel-based sorbents from EFB.

Design/methodology/approach: Hydrogels were synthesised by polymerisation of EFB biochar with acrylamide (AAm) as a monomer, N, N'-Methylenebisacrylamide (MBA) as cross-linker and ammonium persulfate (APS) as initiator, as well as by internal gelation method of sodium alginate, empty fruit bunch (EFB), calcium carbonate ($CaCO_3$), and glucono delta-lactone (GDL). From the alginate hydrogels obtained, xerogels were synthesised via the oven-drying method. Then, EFB-based hydrogel and xerogel sorbents were analysed and compared based on characterisation analysis by using scanning electron microscopy (SEM), Brunauer–Emmett–Teller (BET), Fourier-Transform Infrared Spectroscopy (FTIR), and thermogravimetric analysis (TGA).

Findings: The xerogel-based EFB is a better adsorbent than the hydrogel-based EFB because it has a larger pore volume (0.001449 cm^3/g), larger pore size (63.7987 nm), higher moisture content (7.97%), lower ash content (12.55%), and is more thermally stable.

Research limitations/implications: The research is to compare two new adsorbents, namely Hydrogel and Xerogel, from EFB in terms of their characteristics.

Practical implications: Both adsorbents show a highly toxic material uptake, especially EFB xerogel. This adsorbent is comparable with the other commercialised adsorbent. Thus, this product can be a highly potential adsorbent for gas and wastewater adsorption.

Originality/value: The authenticity results of this article were found to be 15% similar. The novelty of this paper is to compare the two adsorbents, namely hydrogel and xerogel, that originated from EFB.

Keywords: Biomass, Hydrogel, Empty fruit bunch, Xerogel, Sorbent

MATERIALS

1. Introduction

A good, clean, and safe environment are important for humans, animals, and plants. However, the increase in chemical and manufacturing industries has led to a higher number of harmful substances in wastewater and gases produced. Various techniques are used to remove them, such as ion exchange, membrane technology, biological process, and adsorption [1]. Adsorption technique is commonly used for removing pollutants that are resulted from industries, such as uranium adsorption by using salicylaldoxime/poly-dopamine graphene oxide nanocomposites, ammonium adsorption by using various natural clay minerals [2], and arsenic trioxide adsorption by using mineral oxide sorbents [3]. To reduce cost, numerous researchers have focused on producing biomass-based adsorbents, such as activated carbon derived from date seed [4], biocomposite of polyaniline and sodium alginate made with Oscillatoria (OS) biomass [5], and adsorbents made of unburned materials from sawdust, rice husk, olive stones, and herbaceous waste combustion [6].

Biomass resources in Malaysia are mostly generated by the palm oil industry [3]. Biomass from the palm oil industry includes empty fruit bunch (EFB), oil palm trunk (OPT), kernel shells, an oil palm frond (OPF), fibres, and palm oil mill effluent (POME). In the case of EFB, there is an estimation that every 1 tonne of oil palm fresh fruit bunch processed would likely generate 230 kg of EFB [7].

Hydrogels and xerogels are widely used adsorbents to remove contaminants. Some studies combined gels with various types of biochar to improve the adsorption efficiency, utilise biomass wastes, and reduce costs at the same time [8,9]. For example, p(acrylamide)-chicken biochar, p(acrylamide)-wood biochar, and p(acrylamide)-tire biochar hydrogel composites adsorbent to remove organic contaminants from aqueous media [10] and cellulose-based xerogel which is derived from orange trees [11]. Hence, the combination of EFB wastes and each of these gels have a high potential of forming efficient adsorbents that are low in cost with raw materials that are easy to obtain and are environmentally friendly, where they are known as xerogel- and hydrogel-based sorbents from EFB [12].

This study aims to synthesise and characterise new hydrogels and xerogels based on oil palm empty fruit bunches as absorbent applications.

2. Methodology

2.1. Materials

The raw EFB was obtained from the palm oil mail industry in Selangor, whereas the glucono delta-lactone (GDL) was supplied by Alfa/US. Meanwhile, chemicals such as sodium alginate, acrylamide (AAm), N, N′-Methylenebisacrylamide (MBA), ammonium persulfate (APS), and calcium carbonate ($CaCO_3$) are obtained from Reichle & De-Massari (R&M) chemical.

2.2. Methods

Preparation of hydrogel-based EFB

Microwave-assisted pyrolysis

An amount of 200 g of EFB was placed in the quartz reactor with 20wt% moisture content. Subsequently, a microwave-assisted pyrolysis process was conducted to produce Biochar with the power of 1000 W and a frequency of 2450 MHz, as conducted in previous work by [9]. The pyrolysis was done for 30 minutes with a nitrogen flow of 150 mL/min.

Hydrogen peroxide washing pretreatment

An amount of 2 L of 0.1 M H_2O_2 was prepared in a 2-L volumetric flask. Then, 10 g of EFB biochar with 11wt% moisture content was added to 200 mL of prepared H_2O_2 solution in a closed beaker and stirred for 6 hours without any heat applied. Next, the treated EFB biochars were washed repeatedly with distilled water until they reached neutral pH (6-7). Then, the samples were dried by using an oven with the temperature of 80°C for two (2) days, and the final moisture content was 1.3wt%. This method was carried out according to [10] but with minor modifications.

Polymerisation of EFB biochar

An amount of 10 g of AAm was dissolved in 10 mL of distilled water to turn it into an AAm solution. Then, 6 g of EFB biochar and 0.01 g of MBA were added to the solution and mixed thoroughly. Next, 2 mL of 0.703 g of APS aqueous solution was added. After the solution was mixed completely, the EFB hydrogel solution was placed immediately into a plastic mould. Then, it was placed in an oven at 40°C and 30 min for the polymerisation process. Subsequently, the EFB hydrogel solution was solidified and hydrogenised. Finally, they were left to cool for 24 hours at room temperature to allow complete gelation. This method is referred to [10].

Preparation of Xerogel-based EFB

Mechanical pretreatment of EFB

Using a ball mill, the EFB pieces were ground with a frequency of 30 seconds^{-1} for two (2) minutes. The ball mill method was referred to [13] but with minor modifications. Then, using a mixer (model 686CS), the EFBs were ground again at a constant speed of 5000 rpm for 20 minutes. The blended EFBs were then placed through a tray to obtain particulates with sizes smaller than 200 μ.

Preparation of EFB-based sodium alginate composite

0.5 g of sodium alginate was added to 50 ml of distilled water and stirred using a magnetic stirrer. Then, 0.1 g of $CaCO_3$, 0.5 g of grind EFBs, and 0.15 g of GDL were added, one by one, until it was fully homogenised. Then, the solution was transferred to the square mould and placed in the refrigerator for 24 hours. The gel was called alginate hydrogel. Next, the hydrogel was removed from the square mould and placed onto a petri dish. The measurements, such as gel mass and volume, were taken before and after drying, and the shrinkage was 69.24%. This method referred to Co et al. [13] but with some changes.

Oven drying

In order to produce xerogels, the alginate hydrogel was dried via oven drying at 60°C for 24 hours. This process is conducted by using Laboratory Oven Memmert UFP800. This method was done based on the works by [14].

Characterisation analysis

The characterisation analysis of samples was done according to ASTM standards. The surface morphology of samples was done via scanning electron microscopy (SEM-model SU3500). Before the imaging process, the samples were sputter-coated with platinum within 1 minute at 2 MPa of pressure. The surface area, pore volume, and pore size of the materials were characterised by nitrogen adsorption-desorption analysis via Brunauer–Emmett–Teller (BET) 3Flex Micromeritics at a degassed temperature of 120°C under a continuous nitrogen flow of 10 L/min for 24 hours before the analysis. The functional groups of the materials were determined via Fourier-Transform Infrared Spectroscopy (FTIR) analysis using Perkin Elmer Spectrum One FTIR Spectrometer. Thermogravimetric analyser TGA/SDTA51 was used to determine the proximate analysis and thermal stability of raw EFB, hydrogel- and xerogel-based EFB at 600°C and a heating rate of 2°C min^{-1} under nitrogen atmosphere at 25 mL/min flow velocity [15].

In this section, it is necessary to present in detail the assumptions and course of own research to such an extent that a reader could repeat those works if he were going to confirm the achieved results. In short papers, that information should be given in as short a version as possible.

3. Results and discussion

3.1. Surface morphology analysis

The analysis for both gels was taken with different equipment because the characterisation for hydrogel-based EFB was referred to research done. Figures 1 and 2 show the surface morphology of raw EFB via SEM and FESEM, respectively. Generally, the surface area morphology analysis of raw EFB from all magnifications in Figure 1 shows that the whole fibre is rough and firm, with a highly ordered pattern of fibrils. Based on Figures 1a and 1b, the fibres of raw EFB are rough and scattered all over the surface.

Further, based on Figure 1b, it can be seen that a strand of EFB has a rough texture with some cracks on its surface. Figure 2 shows a clearer image of the raw EFB surface where it contains pores. According to [16], lignin removal through Hydrogen Peroxide Washing is the reason behind the cracks and micropores on the strands of EFB.

Next is the analysis surface morphology of xerogel-based EFB, untreated hydrogel-based EFB and pretreated hydrogel-based EFB. Figure 3, Figure 4 and Figure 5 show the SEM image of xerogel-based EFB, FESEM image of untreated hydrogel-based EFB and FESEM image of pretreated hydrogel-based EFB, respectively. Based on Figure 3, most of the EFB fibres were immersed in the alginate surface, which preserved its form and had pores.
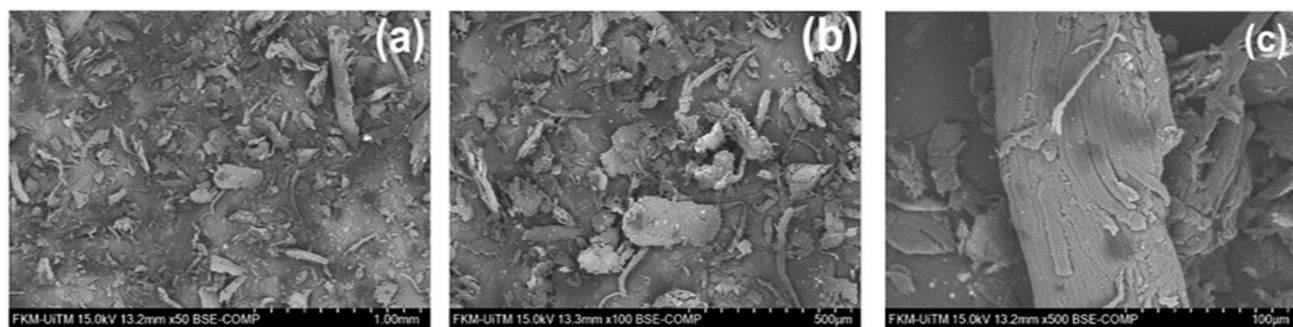
Fig. 1. SEM images of raw EFB from various magnifications: a) 50x; b) 100x; and c) 500x
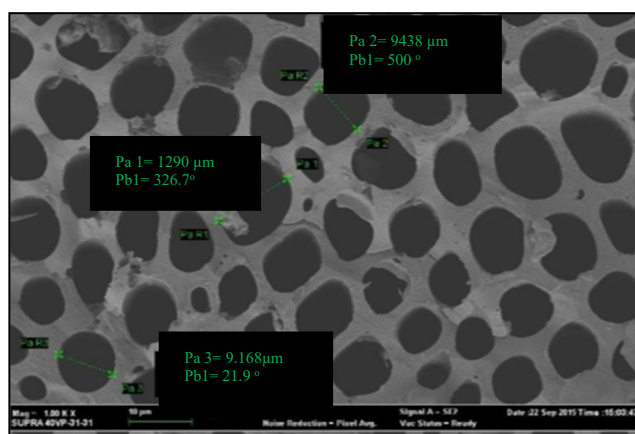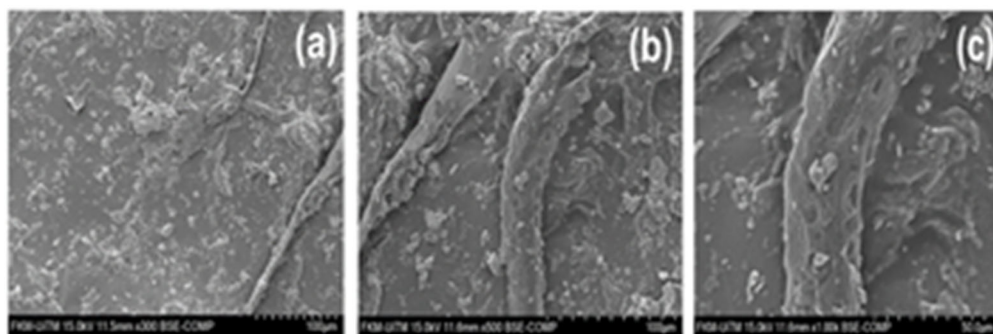

Fig. 2. FESEM image of raw EFB

Fig. 3. SEM image of xerogel-based EFB at various magnifications: a) 300x; b) 500x; and c) 1000x

The surface of the fibres in xerogel-based EFB was brittle due to the properties of xerogel being highly dependent on the solid component and, consequently, the bulk density. The pores show the potential of xerogel EFB as adsorbent material.

Meanwhile, the surface morphology of untreated hydrogel-based EFB in Figure 4 shows that some of the pores were clogged by hydrogel, and more unstable holes were formed holes which is effects form the polymerisation process. However, it may seem like the untreated hydrogel-based EFB had more and larger pores compared to xerogel-based EFB. It can be deduced from this that the hydrogel's potential to swell in the presence of a hydrophilic liquid would assist in removing contaminants trapped in pores and holes.
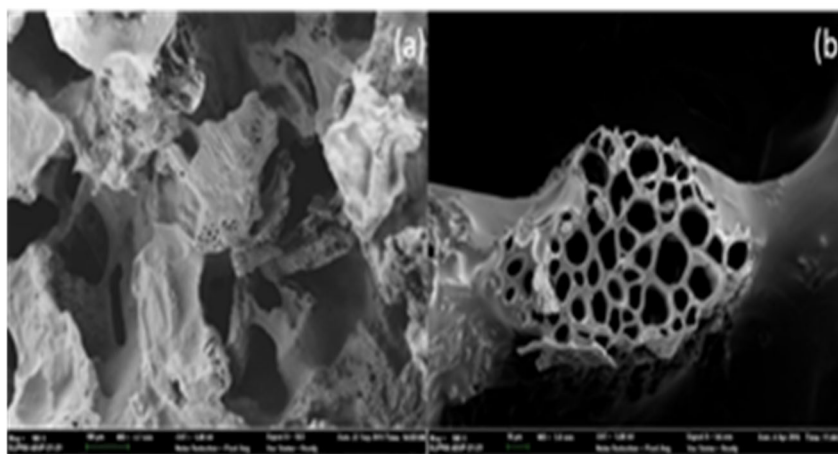
Fig. 4. FESEM image of untreated hydrogel- based EFB at various magnifications: a) 100x; and b) 500x
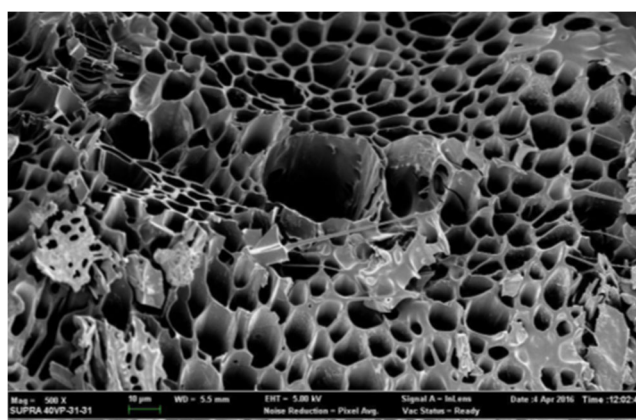

Fig. 5. FESEM image of pretreated hydrogel-based EFB

Hence, it is better to compare the two types of gels after obtaining the BET analysis, as it will measure the pore volume, surface, and pore size. Since both xerogel-based EFB and untreated hydrogel-based EFB showed images of pore existence, this means that both have the potential to be good adsorbents. However, there are still weaknesses with untreated hydrogel-based EFB, such as clogged holes and instability, which are believed to be attributable to the impurities from EFB. To remove impurities that will disrupt the polymerisation process, EFB must undergo chemical pretreatment first. Figure 5 shows the surface morphology of hydrogel-based EFB that was already pretreated by hydrogen peroxide before the polymerisation was done. The image shows that the pretreated hydrogel-based sorbent from EFB had more stable and stronger walls with larger and much more pores than the untreated hydrogel EFB. This is because, as an oxidising agent and one alkaline peroxide,

H_2O_2 pretreatment eliminates the lignin, while the cellulose is selectively retained to reduce the wall thickness of hemicellulose [17,18]. Furthermore, the higher number of pores very well indicates the increased adsorption ability of hydrogel-based EFB. Hence, it is recommended for EFB that is used to synthesise xerogel-based EFB to undergo chemical pretreatment before its internal gelation process to make the walls stronger, increase the number of pores, pore size, and provide higher adsorption potential.

3.2. Brunauer–Emmett–Teller (BET) analysis

Table 1 demonstrates the analysis for Brunauer-Emmett-Teller (BET), which shows the total pore volume, surface area, and pore size of raw EFB, xerogel-based EFB, and hydrogel-based EFB.

Table 1.
BET surface area and porosity analysis for all

Material	BET surface area, m^2/g	Total pore volume, cm^3/g	Average pore size, Å
Raw EFB	1.6061	0.001729	66.6276
Xerogel-based EFB	0.9086	0.001449	63.7987
Hydrogel-based EFB	1.5997	0.000965	38.3805

Based on Table 1, raw EFB has the largest surface area of 1.6061 m^2/mg, pore volume of 0.001729 cm^3/g, and average pore size of 66.6276 nm. Furthermore, xerogel-based EFB has a smaller surface area of 0.9086 m^2/g but a bigger pore volume and pore size of 0.001449 cm^3/g and 63.7987 nm, respectively, compared with hydrogel-based EFB with a surface area of 1.5997 m^2/g, pore volume of 0.000965 cm^3/g, and pore size of 38.3805 nm. The surface area, pore volume, and pore size of EFB decreased after the polymerisation for both types of gels had taken place. Due to the chemicals added to the process, the morphology of EFB changed. Large surface area is usually referred to as a crucial characteristic to enhance the capacity of adsorption because adsorption is a surface reaction [19]. However, the high surface area of the raw EFB may be due to its high volatile matter content. The generation of more pores is due to the volatile release from biomass, where numerous micropores will be created on the surface of the adsorbent [20]. According to The International Union of Pure and Applied Chemistry (IUPAC), macropore materials are those with pore sizes larger than 50 nm. Hence, raw EFB and xerogel-based EFB are macropore materials. Meanwhile, since hydrogel-based EFB has a pore size of 38.3805 nm, it contains most mesopore materials because, according to IUPAC, the range for mesopore materials is in the range of 2 nm to 50 nm. According to [21], the size of the pore does not have a crucial role in absorption because the absorbent still manages to absorb oil, although it has small pore sizes. However, research from [19] stated that pore sizes bigger than 10 nm are good for adsorption, as it allows faster adsorbate transport through the adsorbent. Hence, it can be concluded that both xerogel and hydrogel-based sorbent from EFB may be good for adsorption, as they have pore sizes bigger than 10 nm.

Next, pore volume is also important for adsorption. [21] stated that adsorption capacity is generally expected to increase as the pore volume and specific surface area increase. Cross-linking concentration can affect the pore volume and pore size, which [22] reported that cross-linking density in hydrogel networks is proportionally inverse to the pore size. This is proven by research was done by [12], which produced chitosan (CHI) hydrogel with genipin (Gp) as a cross-linker. The research found that the hydrogel with a lower concentration of genipin had a loosened surface with larger pores compared to the one with a higher concentration of genipin. Hence, a lower concentration of cross-linker is preferable to increase pore volume and specific surface area, which can increase the adsorption ability. In this case, xerogel has a higher pore volume than hydrogel. The conclusion of the BET analysis is although the surface area of xerogel-based EFB is smaller than hydrogel-based EFB, it has a bigger volume and pore size, demonstrating the possibility of xerogel being a better adsorbent than hydrogel.

3.3. Thermogravimetric analysis (TGA)

Figure 6 shows the thermogravimetric analysis (TGA) curve of raw EFB, hydrogel-based EFB, and xerogel-based EFB. According to the TGA curve, the degradation of a material can be observed by the weight loss, starting from a lower temperature which continues until it reaches a high temperature. The weight of the material decreases as the temperature increases, which shows the effect of thermal treatment [23]. To perform a comparison of thermal stability, the TGA curve is divided into three sections. The first section starts from the range of 26°C until 33°C, the second section is from the temperature range of 100°C until 400°C, while the third section is from 900°C until 1100°C. The first section represents the first degradation of moisture, the second section represents the volatile matter, and the last section is the fixed carbon [24,25]. The degradation in the first region for xerogel-based EFB is higher and earlier than raw EFB and hydrogel-based EFB. The weight loss in this section is due to the evaporation of the mixture and low molecular substances [25]. In the first region, the release of moisture in xerogel-based EFB was earlier than raw EFB and hydrogel, respectively. This can be explained by the observation that xerogel's crystallinity increases due to the -OH groups being replaced by intermolecular hydrogen bonds, which decrease moisture absorption [24]. For the next section, the earliest to degrade is xerogel at a temperature of 393.21°C, with only a little difference with raw EFB, which degraded at 401.79°C, but there is a clear difference with hydrogel-based EFB at 461.31°C.
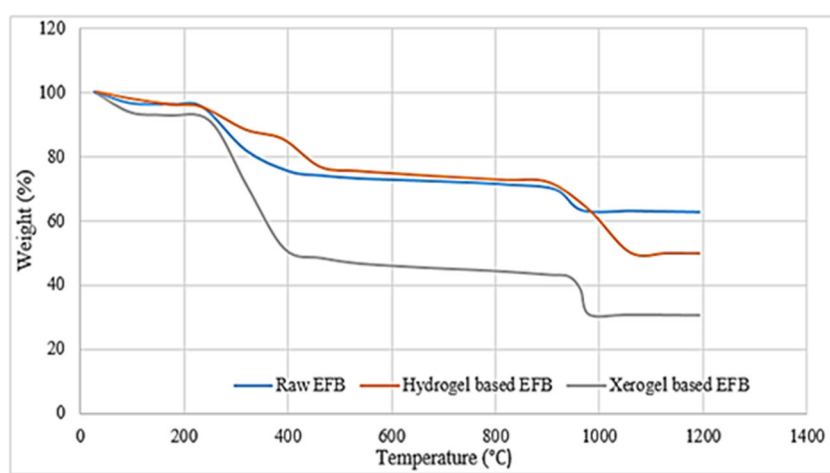
Fig. 6. Thermogravimetry analysis (TGA) curve study

Table 2.
Proximate analysis

Material	Moisture Content, %	Volatile Content, %	Fixed Carbon Content, %	Ash Content, %
Raw EFB	3.73	69.44	6.44	20.39
Hydrogel-based EFB	4.47	24.53	21.00	50.00
Xerogel-based EFB	7.97	64.71	45.02	12.55

Moreover, the weight loss of xerogel is higher compared with others. This is due to the breakdown of the alginate backbone and the massive loss of hydroxyl groups on the water-form alginate. For the third section, the earliest to degrade is raw EFB at the temperature of about 900°C, followed by xerogel at a similar range and hydrogel at a temperature of more than 1000°C. Xerogel-based EFB has a higher weight loss and is more thermally stable than hydrogel-based EFB.

Table 2 shows the proximate analysis of raw EFB, hydrogel-based EFB, and xerogel-based EFB regarding ash, moisture, volatile, and fixed carbon contents. The reason for proximate analysis is to establish the ratio of combustible, represented by volatile matter and fixed carbon, to incombustible, which is then represented by moisture and ash substances in the materials because the ratio will be beneficial to delineating their energy content [26].

The moisture content of EFB in this study is between the range of EFB moisture content provided by [26], which is from 2.40% to 14.28%. Moreover, the volatile content for raw EFB, 69.44%, is almost similar to [27], which has a value of 69.95%. The fixed carbon content of raw EFB used in this study is 6.44%, which is rather similar to the raw EFB result from [8, 28] with 5.7% of fixed carbon content. Meanwhile, the ash content of raw EFB in this study,

20.39%, is around the same value as the ash content of raw EFB from [29] with a value of 20.48%. Based on Table 2, raw EFB has the lowest moisture content (3.73%) compared with hydrogel- and xerogel-based EFB. This is because of the cross-linking process that took place for both types of gels. For both cross-linking processes, water was added, which is believed to be the reason for the increased moisture content. The amount of volatile content of raw EFB, which is 69.44%, is higher than both hydrogel- and xerogel-based EFB, which are 24.53% and 64.71%, respectively. Hydrogel has the lowest volatile content, and this is because, before the polymerisation process, the raw EFB went through a pyrolysis process which was conducted at a high temperature where a lot of volatile matter contents were released [30].

In addition, there was hydrogen peroxide pre-washing to remove volatile contents from EFB used for hydrogel. Moreover, there is an increasing trend for fixed carbon of raw EFB (6.44%) to hydrogel-based EFB (21%) and xerogel-based EFB (45.02%). According to [29], this increment may be because of the devolatilisation and decomposition reaction that occurred. Next, ash content is reduced from raw EFB (20.39%) to xerogel-based EFB (12.55%). Ironically, it differs from hydrogel-based EFB, which showed higher ash content (50%). The increment of ash content in the hydrogel is also because of the pyrolysis that transpired.
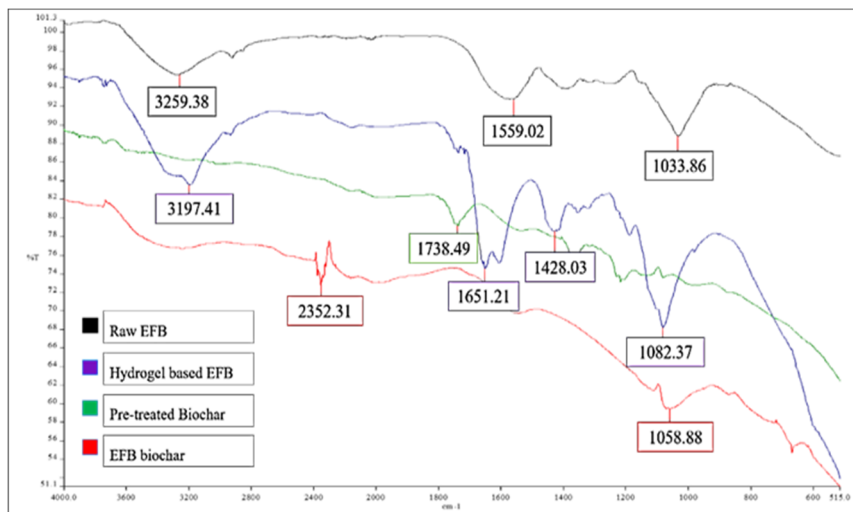
Fig. 7. FTIR spectrum for hydrogel-based EFB

In summary, the proximate analysis shows that xerogel-based EFB has more advantages as an adsorbent because it has greater moisture content and lowers ash content than hydrogel-based EFB. Adsorbents with higher moisture content are preferable because the adsorption capability will be higher. According to [31], when there is only a little moisture content in adsorbents, the adsorption of moisture by the adsorbents is also less. In contrast, the ash contents are preferred to be low for good adsorption. This is because too much ash content can clog the pores of the adsorbent, which will lead to a reduction of its surface area [32]. Besides that, based on research from [31], ash content may cause the increment of hydrophilicity, which is not good for adsorbents. However, hydrogel-based EFB has lesser volatile content than xerogel-based EFB. This may be due to the pretreatment that helped to reduce volatile matters, such as pyrolysis and hydrogen peroxide pre-washing of EFB. High volatile matter content is not good for adsorbents, as it will disrupt the adsorption process.

3.4. Fourier-Transform Infrared Spectroscopy (FTIR)

Figure 7 shows the FTIR spectrum for hydrogel-based EFB, raw EFB, EFB biochar, and biochar pretreated with hydrogen peroxide. The presence of O-H stretching is represented by the raw EFB spectrum, which shows a broad characteristic peak at 3259.38 cm^{-1}. This O-H stretching indicates the existence of phenols and alcohols [33]. The reason for O-H stretching is because of moisture content in the fibres, in which hydroxyl groups are found in the form of lignin, hemicellulose, and cellulose [34,35]. EFB biochar shows stretching of O= C= O, which is CO_2 at the wavelength of 2352.1 cm^{-1}. The existence of CO_2 has resulted from pyrolysis process where it usually produces a gaseous product, which has high CO_2 content [36]. The presence of CO_2 in EFB biochar is from the pyrolysis process, which is generally produced gaseous products rich in CO_2. The CO_2 formed was removed after hydrogen peroxide treatment, as shown on the spectrum of pretreated biochar. This is because hydrogen peroxide can remove volatile materials, such as CO_2. There is low transmittance based on the peaks shown by hydrogel-based EFB, which indicates a strong absorption capability. The peak of hydrogel-based EFB at 3197.41 cm^{-1} indicates that there is O-H stretching, which means there are phenols and alcohols in the structure. Besides, hydrogel-based EFB also shows some changes in the functional group after the cross-linking process. The peaks of 1651 cm^{-1} and 1082 cm^{-1} show the presence of C=C stretching, which indicates conjugate alkene; and C-N stretching, which represents amine [37].

The FTIR spectrum for raw EFB and xerogel-based EFB is shown in Figure 8. The presence of O-H stretching is confirmed as both spectrums of raw EFB and xerogel-based EFB illustrated a peak at 3335 cm^{-1} and 3323 cm^{-1}, respectively. This indicates the presence of alcohol and phenols in both materials [38]. There is C=O stretching indicated at 1735 cm^{-1} of xerogel. This means that there is the existence of hemicellulose and lignin. This stretching is believed to be caused by xerogel's cross-linking and drying technique [39]. The peak at 1031 cm^{-1} at the raw EFB spectrum indicates the presence of C-O stretching, while the peak of 1053 cm^{-1} at the xerogel-based EFB spectrum shows the characteristics of anhydrous glucose chains [35].
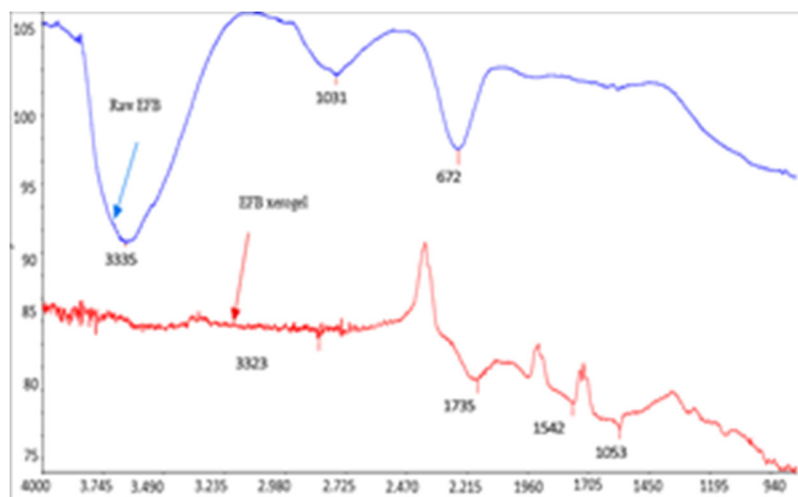
Fig. 8. FTIR spectrum for xerogel-based EFB

4. Conclusions

In summary, based on the results of the characterisation analysis of xerogels and hydrogel-based EFB via scanning electron microscopy (SEM), Brunauer–Emmet–Teller (BET), thermogravimetric analysis (TGA), and Fourier-Transform Infrared Spectroscopy (FTIR) analysis, both types of gels have shown characteristics of being good adsorbents. This means that empty fruit bunches (EFB) are one of the agricultural wastes suitable for developing into adsorbents with high adsorption capability. According to BET and TGA analysis, xerogel-based EFB is a better adsorbent than hydrogel-based EFB because it has larger pore volume and pore size, higher moisture content, and lower ash content, and is more thermally stable. However, hydrogel-based EFB has lower volatile content compared to xerogel-based EFB. This might be because hydrogel-based EFB went through pre-treatment, such as hydrogen peroxide pre-washing and pyrolysis, which removed the content of the volatile material. Meanwhile, xerogel-based EFB did not undergo any pre-treatment process, except for the grinding process, which was done to reduce the size of raw EFB. Hence, it is believed that if xerogel-based EFB undergoes suitable pre-treatment before the cross-linking process, it will reduce volatile materials and increase its adsorptive abilities.

Acknowledgements

Additional information

The article was presented at the 5th ICET 2021: 5th International Conference on Engineering Technology Virtual Conference KEMAMAN, Malaysia, October 25-26, 2021.

References

[1] Y. Qian, Y. Yuan, H. Wang, H. Liu, J. Zhang, S. Shi, Z. Guo, N. Wang, Highly efficient uranium adsorption by salicylaldoxime/polydopamine graphene oxide nanocomposites, Journal of Materials Chemistry A 6/48 (2018) 24676-24685.
DOI: https://doi.org/10.1039/C8TA09486A

[2] A. Alshameri, H. He, J. Zhu, Y. Xi, R. Zhu, L. Ma, Q. Tao, Adsorption of ammonium by different natural clay minerals: Characterisation, kinetics and adsorption isotherms, Applied Clay Science 159 (2017) 83-93.
DOI: https://doi.org/10.1016/j.clay.2017.11.007

[3] S. Yu, C. Zhang, L. Ma, Q. Fang, G. Chen, Insight into As_2O_3 adsorption characteristics by mineral oxide

sorbents: Experimental and DFT study, Chemical Engineering Journal 420/2 (2021) 127593. DOI: https://doi.org/10.1016/j.cej.2020.127593

[4] A.E. Ogungbenro, D.V. Quang, K.A. Al-Ali, L.F. Vega, M.R.M. Abu-Zahra, Synthesis and characterisation of activated carbon from biomass date seeds for carbon dioxide adsorption, Journal of Environmental Chemical Engineering 8/5 (2020) 104257.
DOI: https://doi.org/10.1016/j.jece.2020.104257

[5] M. Maqbool, H.N. Bhatti, S. Sadaf, M.M. Al-anazy, M. Iqbal, Biocomposite of polyaniline and sodium alginate with Oscillatoria biomass: a potential adsorbent for the removal of basic blue 41, Journal of Materials Research and Technology 9/6 (2020) 14729-14741. DOI: https://doi.org/10.1016/j.jmrt.2020.10.017

[6] J.F. Saldarriaga, N.A. Montoya, I. Estiati, A.T. Aguayo, R. Aguado, M. Olazar, Unburned material from biomass combustion as low-cost adsorbent for amoxicillin removal from wastewater, Journal of Cleaner Production 284 (2021) 124732. DOI: https://doi.org/10.1016/j.jclepro.2020.124732

[7] R.T.L. Ng, D.K.S. Ng, Systematic Approach for Synthesis of Integrated Palm Oil Processing Complex. Part 1: Single Owner, Industrial and Engineering Chemistry Research 52/30 (2013) 10206-10220. DOI: https://doi.org/10.1021/ie302926q

[8] P. Kimia, B. Tandan, K. Buah, K. Sawit, Chemical and Physical Characterization of Oil Palm Empty Fruit Bunch, Malaysian Journal of Analytical Sciences 21/1 (2017) 188-196. DOI: http://dx.doi.org/10.17576/mjas-2017-2101-22

[9] N.B. Juli, N. Talib, N. Ahmad, A.B. Alias, Monte carlo simulation hydrogen sulphide gas adsorption by using hydrogel biochar, Egyptian Journal of Chemistry 64/6 (2021) 2789-2796.
DOI: https://doi.org/10.21608/ejchem.2021.54278.3129

[10] N. Karakoyun, S. Kubilay, N. Aktas, O. Turhan, M. Kasimoglu, S. Yilmaz, N. Sahiner, Hydrogel – Biochar composites for effective organic contaminant removal from aqueous media, Desalination 280/1-3 (2011) 319-325. DOI: https://doi.org/10.1016/j.desal.2011.07.014

[11] S. Rbihi, L. Laallam, M. Sajieddine, A. Jouaiti, Characterisation and thermal conductivity of cellulose based composite xerogels, Heliyon 5/5 (2019) e01704. DOI: https://doi.org/10.1016/j.heliyon.2019.e01704

[12] L. Gao, H. Gan, Z. Meng, R. Gu, Z. Wu, L. Zhang, X. Zhu, W. Sun, J. Li, Y. Zheng, G. Dou, Colloids and Surfaces B : Biointerfaces Effects of genipin cross-linking of chitosan hydrogels on cellular adhesion and

viability, Colloids and Surfaces B: Biointerfaces 117 (2014) 398-405.
DOI: https://doi.org/10.1016/j.colsurfb.2014.03.002

[13] M.R. Zakaria, S. Fujimoto, S. Hirata, M.A. Hassan, Ball Milling Pretreatment of Oil Palm Biomass for Enhancing Enzymatic Hydrolysis, Applied Bio-chemistry and Biotechnology 173 (2014) 1778-1789. DOI: https://doi.org/10.1007/s12010-014-0964-5

[14] R. Rodríguez-Dorado, C. López-Iglesias, C.A. García-González, G. Auriemma, R.P. Aquino, P. Del Gaudio, Design of Aerogels, Cryogels and Xerogels of Alginate: Effect of Molecular Weight, Gelation Conditions and Drying Method on Particles' Micromeritics, Molecules 24/6 (2019) 1049. DOI: https://doi.org/10.3390/molecules24061049

[15] N.H. Meri, Adsorption Of Hydrogen Sulphide (H_2S) By Empty Fruit Bunch Hydrogel Biochar Composite (EFB-HBC), MSc Thesis, Universiti Teknologi Mara (UiTM), Malaysia, 2019.

[16] N.F.A.A. Rizal, M.F. Ibrahim, M.R. Zakaria, E.K. Bahrin, S. Abd-Aziz, M.A. Hassan, Combination of superheated steam with laccase pretreatment together with size reduction to enhance enzymatic hydrolysis of oil palm biomass, Molecules 23/4 (2018) 811. DOI: https://doi.org/10.3390/molecules23040811

[17] V.S. Prabhin, K. Jeyasubramanian, N.R. Romulus, N.N. Singh, Fabrication of dye sensitized solar cell using chemically tuned CuO nanoparticles prepared by sol-gel method, Archives of Materials Science and Engineering 83/1 (2017) 5-9.
DOI: https://doi.org/10.5604/01.3001.0009.7535

[18] D.Q. A'yuni, A. Subagio, H. Hadiyanto, A.C. Kumoro, M. Djaeni, Microstructure silica leached by naoh from semi-burned rice husk ash for moisture adsorbent, Archives of Materials Science and Engineering 108/1 (2021) 5-15.
DOI: https://doi.org/10.5604/01.3001.0015.0248

[19] P. Suresh, L. Korving, K.J. Keesman, M.C.M. Van Loosdrecht, G. Witkamp, Effect of pore size distribution and particle size of porous metal oxides on phosphate adsorption capacity and kinetics, Chemical Engineering Journal 358 (2019) 160-169. DOI: https://doi.org/10.1016/j.cej.2018.09.202

[20] R.E. Masto, A. Ansari, J. George, V.A. Selvi, L.C. Ram, Co-application of biochar and lignite fly ash on soil nutrients and biological parameters at different crop growth stages of Zea mays. Ecological Engineering 58 (2013) 314-322.
DOI: https://doi.org/10.1016/j.ecoleng.2013.07.011

[21] N.M.F. Mat Yasin, Synthesis and Characterisation of Oven-Dried Oil Palm Empty Fruit Bunches-Based Xerogels for Absorption of Engine Oil, MSc Thesis, Universiti Teknologi Mara (UiTM), Malaysia, 2021.

[22] P.N. Dave, A. Gor, Natural Polysaccharide-Based Hydrogels and Nanomaterials: Recent Trends and Their Applications, in: C.M. Hussain (ed), In Micro and Nano Technologies, Handbook of Nanomaterials for Industrial Applications, Elsevier, 2018, 36-66. DOI: https://doi.org/10.1016/B978-0-12-813351-4.00003-1

[23] A. Sarfraz, A. H. Raza, M. Mirzaeian, Q. Abbas, R. Raza, Electrode Materials for Fuel Cells, in: A.-G. Olabi (ed), Encyclopedia of Smart Materials, Volume 2, Elsevier, 2022, 341-356.
DOI: https://doi.org/10.1016/B978-0-12-803581-8.11742-4

[24] N.H. Meri, A.B. Alias, N. Talib, Z.A. Rashid, W.A.W.A.K. Ghani, Comparison of H_2S adsorption by two hydrogel composite (HBC) derived by Empty Fruit Bunch (EFB) biochar and Coal Fly Ash (CFA), IOP Conference Series: Materials Science and Engineering 334 (2018) 012038.
DOI: https://doi.org/10.1088/1757-899X/334/1/012038

[25] M.A.F. Supian, K.N.M. Amin, S.S. Jamari, S. Mohamad, Production of cellulose nanofiber (CNF) from empty fruit bunch (EFB) via mechanical method, Journal of Environmental Chemical Engineering 8/1 (2020) 103024.
DOI: https://doi.org/10.1016/j.jece.2019.103024

[26] S.H. Chang, An overview of empty fruit bunch from oil palm as feedstock for bio-oil production, Biomass and Bioenergy 62 (2014) 174-181.
DOI: https://doi.org/10.1016/j.biombioe.2014.01.002

[27] R. Idris, W.W.F. Chong, A. Ali, S. Idris, M.S. Hasan, F.N. Ani, C.T. Chong, Phenol-rich bio-oil derivation via microwave-induced fast pyrolysis of oil palm empty fruit bunch with activated carbon, Environmental Technology and Innovation 21 (2021) 101291.
DOI: https://doi.org/10.1016/j.eti.2020.101291

[28] T. Nuraiti, T. Izhar, Adsorption of Hydrogen Sulfide (H_2S) from Municipal Solid Waste by Using Biochars, Biointerface Research in Applied Chemistry 12/6 (2022) 8057-8069.
DOI: https://doi.org/10.33263/BRIAC126.80578069

[29] N.M.F.M. Yasin, N.H. Meri, N. Talib, W.A.W.A.K. Ghani, Z.A. Rashid, A.B. Alias, Breakthrough Analysis of Empty Fruit Bunch-Based Hydrogel Biochar Composite (EFB-HBC) for Hydrogen Sulphide (H_2S)

Adsorption Study Removal, in: Advances in Engineering Research, Volume 200, Proceedings of the Third International Conference on Separation Technology 2020 "ICoST 2020", 216-225. DOI: https://doi.org/10.2991/aer.k.201229.030

[30] P. Wahyuningsih, N. Yusri, Hamdani, Characterisation of Activated Carbon Prepared from Oil Palm Empty Fruit Bunch by Chemical Activation using Sulphuric Acid (H_2SO_4), Proceedings of the International Conference on Engineering and Science for Research and Development "ICESReD", 2016, 239-244.

[31] D. Kibami, C. Pongener, K.S. Rao, D. Sinha, Preparation and characterisation of activated carbon from Fagopyrum esculentum Moench by HNO_3 and H_3PO_4 chemical activation, Der Chemica Sinica 5/4 (2014) 46-55.

[32] S. Maulina, M Iriansyah, Characteristics of activated carbon resulted from pyrolysis of the oil palm fronds powder, IOP Conference Series: Materials Science and Engineering 309 (2018) 012072.
DOI: https://doi.org/10.1088/1757-899X/309/1/012072

[33] N. Claoston, A.W. Samsuri, M.A. Husni, M.M. Amran, Effects of pyrolysis temperature on the physicochemical properties of empty fruit bunch and rice husk biochars, Waste Management and Research 32/4 (2014) 331-339.
DOI: https://doi.org/10.1177/0734242X14525822

[34] H.P.S.A. Khalil, A.F.I. Yusra, A.H. Bhat, M. Jawaid, Cell wall ultrastructure, anatomy, lignin distribution, and chemical composition of Malaysian cultivated kenaf fiber, Industrial Crops and Products 31/1 (2010) 113-121.
DOI: https://doi.org/10.1016/j.indcrop.2009.09.008

[35] I.Y.A. Fatah, H.P.S.A. Khalil, M.S. Hossain, A.A. Aziz, Y. Davoudpour, R. Dungani, A. Bhat, Exploration of a chemo-mechanical technique for the isolation of nanofibrillated cellulosic fiber from oil palm empty fruit bunch as a reinforcing agent in composites materials, Polymers 6/10 (2014) 2611-2624. DOI: https://doi.org/10.3390/polym6102611

[36] N.H. Meri, A.B. Alias, Z.A. Rashid, W.A.W.A.K. Ghani, Effect of Chemical Washing Pre-treatment of Empty Fruit Bunch (EFB) biochar on Characterization of Hydrogel Biochar composite as Bioadsorbent, IOP Conference Series: Materials Science and Engineering 358 (2018) 012018. DOI: https://doi.org/10.1088/1757-899X/358/1/012018

[37] E. David, C. Sandru, A. Armeanu, Zeolitization characteristics of fly ash and its use to manufacture

porous materials, Archives of Materials Science and Engineering 90/2 (2018) 56-67.
DOI: https://doi.org/10.5604/01.3001.0012.0663

[38] M. Szindler, M.M. Szindler, L.A. Dobrzański, T. Jung, NiO nanoparticles prepared by the sol-gel method for a dye sensitised solar cell applications, Archives of

Materials Science and Engineering 92/1 (2018) 15-21.
DOI: https://doi.org/10.5604/01.3001.0012.5507

[39] F. Fahma, I. Febiyanti, N. Lisdayana, I.W. Arnata, D. Sartika, Nanocellulose as a new sustainable material for various applications: A review, Archives of Materials Science and Engineering 109/2 (2021) 49-64. DOI: https://doi.org/10.5604/01.3001.0015.2624